

# We are IntechOpen, the world's leading publisher of Open Access books Built by scientists, for scientists

6,900

Open access books available

186,000

International authors and editors

200M

Downloads

Our authors are among the

154

Countries delivered to

TOP 1%

most cited scientists

12.2%

Contributors from top 500 universities



WEB OF SCIENCE™

Selection of our books indexed in the Book Citation Index  
in Web of Science™ Core Collection (BKCI)

Interested in publishing with us?  
Contact [book.department@intechopen.com](mailto:book.department@intechopen.com)

Numbers displayed above are based on latest data collected.  
For more information visit [www.intechopen.com](http://www.intechopen.com)



# Strength and Microstructure of Cement Stabilized Clay

Suksun Horpibulsuk  
*Suranaree University of Technology,  
Thailand*

## 1. Introduction

The soil/ground improvement by cement is an economical and worldwide method for pavement and earth structure works. Stabilization begins by mixing the in-situ soil in a relatively dry state with cement and water specified for compaction. The soil, in the presence of moisture and a cementing agent becomes a modified soil, i.e, particles group together because of physical-chemical interactions among soil, cement and water. Because this occurs at the particle level, it is not possible to get a homogeneous mass with the desired strength. Compaction is needed to make soil particles slip over each other and move into a densely packed state. In this state, the soil particles can be welded by chemical (cementation) bonds and become an engineering material (Horpibulsuk et al., 2006). To reduce the cost of ground improvement, the replacement of the cement by waste materials such as fly ash and biomass ash is one of the best alternative ways. In many countries, the generation of these waste materials is general far in excess of their utilization. A feasibility study of utilizing these ashes (waste materials) to partially replace Type I Portland cement is thus interesting.

The effects of some influential factors, i.e., water content, cement content, curing time, and compaction energy on the laboratory engineering characteristics of cement-stabilized soils have been extensively researched (Clough et al., 1981; Kamon & Bergado, 1992; Yin & Lai, 1998; Miura et al., 2001; Horpibulsuk & Miura, 2001; Horpibulsuk et al., 2003, 2004a, 2004b, 2005, 2006, 2011a). The field mixing effect such as installation rate, water/cement ratio and curing condition on the strength development of cemented soil was investigated by Nishida et al. (1996) and Horpibulsuk et al. (2004c, 2006 and 2011b). Based on the available compression and shear test results, many constitutive models were developed to describe the engineering behavior of cemented clay (Gens and Nova, 1993; Kasama et al., 2000; Horpibulsuk et al., 2010a; Suebsuk et al., 2010 and 2011). These investigations have mainly focused on the mechanical behavior that is mainly controlled by the microstructure. The structure is fabric that is the arrangement of the particles, clusters and pore spaces in the soil as well as cementation (Mitchell, 1993). It is thus vital to understand the changes in engineering properties that result from the changes in the influential factors.

This chapter attempts to illustrate the microstructural changes in cement-stabilized clay to explain the different strength development according to the influential factors, i.e., cement content, clay water content, fly ash content and curing time. The unconfined compressive

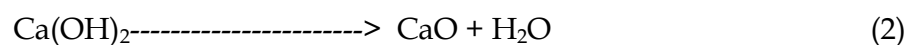
strength was used as a practical indicator to investigate the strength development. The microstructural analyses were performed using a scanning electron microscope (SEM), mercury intrusion porosimetry (MIP), and thermal gravity (TG) tests. For SEM, the cement stabilized samples were broken from the center into small fragments. The SEM samples were frozen at  $-195^{\circ}\text{C}$  by immersion in liquid nitrogen for 5 minutes and evacuated at a pressure of 0.5 Pa at  $-40^{\circ}\text{C}$  for 5 days (Miura et al., 1999; and Yamadera, 1999). All samples were coated with gold before SEM (JEOL JSM-6400) analysis.

Measurement on pore size distribution of the samples was carried out using mercury intrusion porosimeter (MIP) with a pressure range from 0 to 288 MPa, capable of measuring pore size diameter down to 5.7 nm (0.0057 micron). The MIP samples were obtained by carefully breaking the stabilized samples with a chisel. The representative samples of 3-6 mm pieces weighing between 1.0-1.5 g were taken from the middle of the cemented samples. Hydration of the samples was stopped by freezing and drying, as prepared in the SEM examination. Mercury porosimetry is expressed by the Washburn equation (Washburn, 1921). A constant contact angle ( $\theta$ ) of  $140^{\circ}$  and a constant surface tension of mercury ( $\gamma$ ) of 480 dynes/cm were used for pore size calculation as suggested by Eq.(1)

$$D = -(4\gamma\cos\theta) / P \quad (1)$$

where  $D$  is the pore diameter (micron) and  $P$  is the applied pressure (MPa).

Thermal gravity (TG) analysis is one of the widely accepted methods for determination of hydration products, which are crystalline  $\text{Ca}(\text{OH})_2$ , CSH, CAH, and CASH, ettringite (Aft phases), and so on (Midgley, 1979). The CSH, CAH, and CASH are regarded as cementitious products.  $\text{Ca}(\text{OH})_2$  content was determined based on the weight loss between  $450$  and  $580^{\circ}\text{C}$  (El-Jazairi and Illston, 1977 and 1980; and Wang et al., 2004) and expressed as a percentage by weight of ignited sample. When heating the samples at temperature between  $450$  and  $580^{\circ}\text{C}$ ,  $\text{Ca}(\text{OH})_2$  is decomposed into calcium oxide (CaO) and water as in Eq. (2).



Due to the heat, the water is lost, leading to the decrease in overall weight. The amount of  $\text{Ca}(\text{OH})_2$  can be approximated from this lost water by Equation (2), which is 4.11 times the amount of lost water (El-Jazairi and Illston, 1977 and 1980). The change of the cementitious products can be expressed by the change of  $\text{Ca}(\text{OH})_2$  since they are the hydration products.

## 2. Compaction and strength characteristics of cement stabilized clay

Compaction characteristics of cement stabilized clay are shown in Figure 1. The clay was collected from the Suranaree University of Technology campus in Nakhon Ratchasima, Thailand. It is composed of 2% sand, 45% silt and 53% clay. Its specific gravity is 2.74. The liquid and plastic limits are approximately 74% and 27%, respectively. Based on the Unified Soil Classification System (USCS), the clay is classified as high plasticity (CH). It is found that the maximum dry unit weight of the stabilized samples is higher than that of the unstabilized samples whereas their optimum water content is practically the same. This characteristic is the same as that of cement stabilized coarse-grained soils as reported by Horpibulsuk et al. (2006). The adsorption of  $\text{Ca}^{2+}$  ions onto the clay particle surface

decreases the repulsion between successive diffused double layers and increases edge-to-face contacts between successive clay sheets. Thus, clay particles flocculate into larger clusters, which increases in the plastic limit with an insignificant change in the liquid limit (*vide* Table 1). As such, the plasticity index of the mixture decreases due to the significant increase in the plastic limit. Because the *OWC* of low swelling clays is mainly controlled by the liquid limit (Horpibulsuk et al., 2008 and 2009), the *OWCs* of the unstabilized and the stabilized samples are almost the same (*vide* Table 1). Figure 2 shows the compaction curve of the fly ash (FA) blended cement stabilized clay for different replacement ratios (ratios of cement to fly ash, C:F) compared with that of the unstabilized clay. Two fly ashes are presented in the figure: original, OFA ( $D_{50} = 0.03$  mm) and classified, CFA ( $D_{50} = 0.009$  mm) fly ashes. It is noted that the compaction curve of the stabilized clay is insignificantly dependent upon replacement ratio and fly ash particles. Maximum dry unit weight of the stabilized clay is higher than that of the unstabilized clay whereas their optimum water content is practically the same.

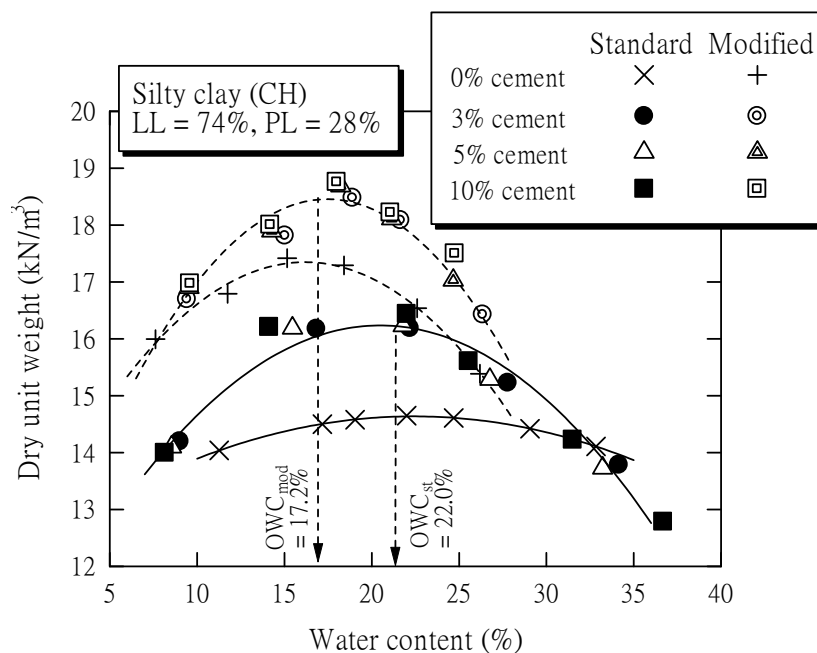


Fig. 1. Plots of dry unit weight versus water content of the uncemented and the cemented samples compacted under standard and modified Proctor energies (Horpibulsuk et al., 2010b)

Cement (%)	Atterberg's limits (%)			OWC (%)		$\gamma_{dmax}$ (kN/m <sup>3</sup> )	
	LL	PL	PI	Std.	Mod.	Std.	Mod.
0	74.1	27.5	46.6	22.4	17.2	14.6	17.4
3	74.1	45.0	29.1	22.2	17.5	16.2	18.5
5	72.5	45.0	27.5	21.8	17.3	16.2	18.7
10	71.0	44.8	26.2	22.0	17.4	16.4	18.8

Table 1. Basic properties of the cemented samples

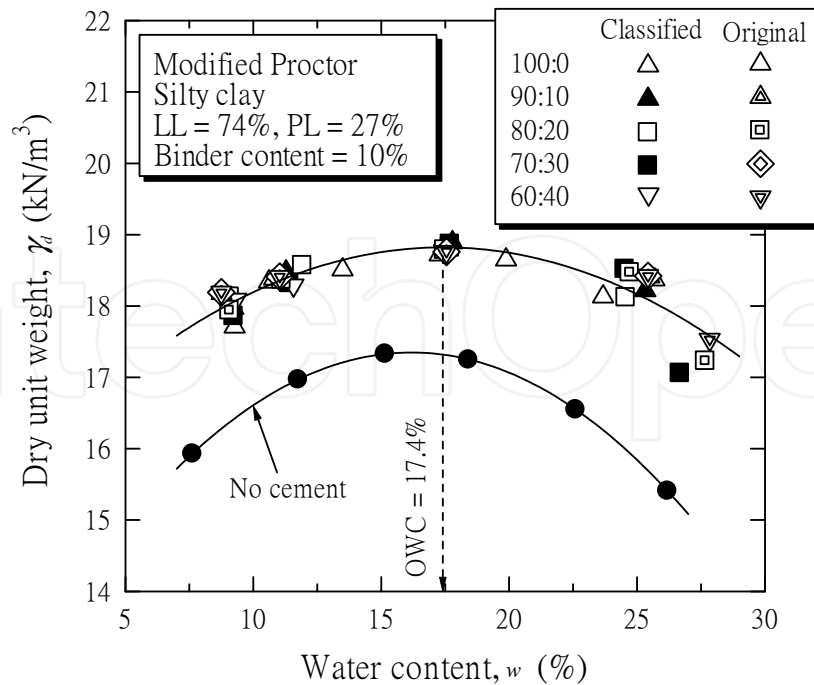


Fig. 2. Compaction curves of the OFA and CFA blended cement stabilized clay and the unstabilized clay (Horpibulsuk et al., 2009)

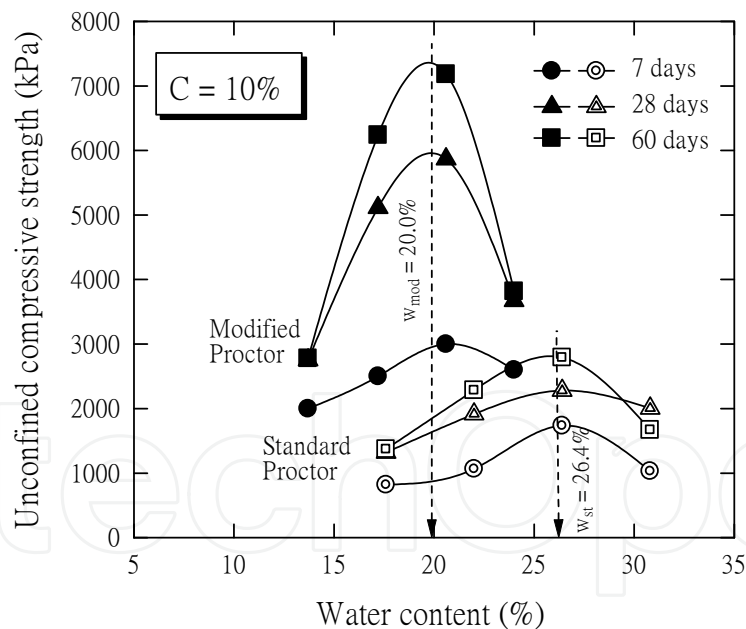


Fig. 3. Effect of compaction energy and curing time on strength development (Horpibulsuk et al., 2010b)

Typical strength-water content relationships for different curing times and compacton energies of the stabilized samples are shown in Figure 3. The strength of the stabilized samples increases with water content up to 1.2 times the optimum water content and decreases when the water content is on the wet side of optimum. At a particular curing time, the strength curve depends on the compaction energy. As the compaction energy increases, the maximum strength increases and the water content at maximum strength decreases. For

the same compaction energy, the strength curves follow the same pattern for all curing times, which are almost symmetrical around 1.2OWC for the range of the water content tested. Figure 4 shows the strength versus water content relationship of the CFA blended cement stabilized clay at different replacement ratios after 60 days of curing compared with that of the unstabilized clay. The maximum strengths of the stabilized clay are at about 1.2OWC whereas the maximum strength of the unstabilized clay is at OWC (maximum dry unit weight). This is because engineering properties of unstabilized clay are mainly dependent upon the densification (packing).

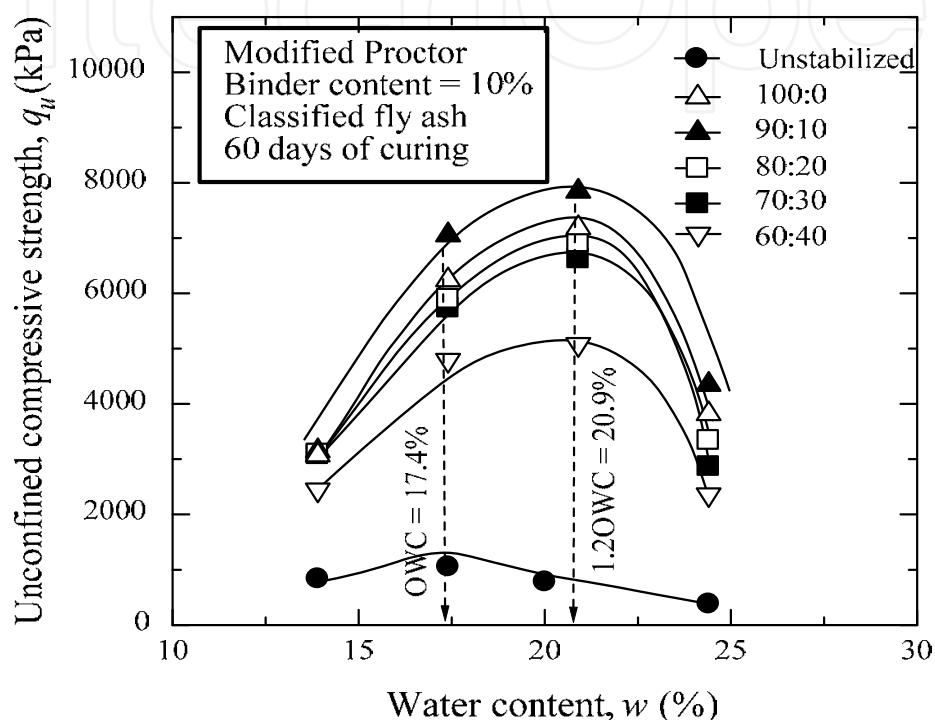


Fig. 4. Strength versus water content relationship of the CFA blended cement stabilized clay at different replacement ratios and 60 days of curing (Horpibulsuk et al., 2009)

Figure 5 shows the strength development with cement content (varied over a wide range) of the stabilized samples compacted under the modified Proctor energy at 1.2 OWC (20%) after 7 days of curing. The strength increase can be classified into three zones. As the cement content increases, the cement per grain contact point increases and, upon hardening, imparts a commensurate amount of bonding at the contact points. This zone is designated as the *active zone*. Beyond this zone, the strength development slows down while still gradually increasing. The incremental gradient becomes nearly zero and does not make any further significant improvement. This zone is referred to as the *inert zone* ( $C = 11-30\%$ ). The strength decrease appears when  $C > 30\%$ . This zone is identified as the *deterioration zone*.

Influence of replacement ratio on the strength development of the blended cement stabilized clay compacted at water content ( $w$ ) of 1.2OWC ( $w = 20.9\%$ ) for the five curing times is presented in Figure 6. For all curing times, the samples with 20% replacement ratio exhibit almost the same strength as those with 0% replacement ratio. The 30 and 40% replacement samples exhibit lower strength than 0% replacement samples. The samples with 10% replacement ratio exhibit the highest strength since early curing time. The sudden strength

development with time is not found for all replacement ratios. This finding is different from concrete technology where the role of fly ash as a pozzolanic material comes into play after a long curing time (generally after 60 days). In other words, the strength of concrete mixed with fly ash is higher than that without fly ash after about 60 days of curing.

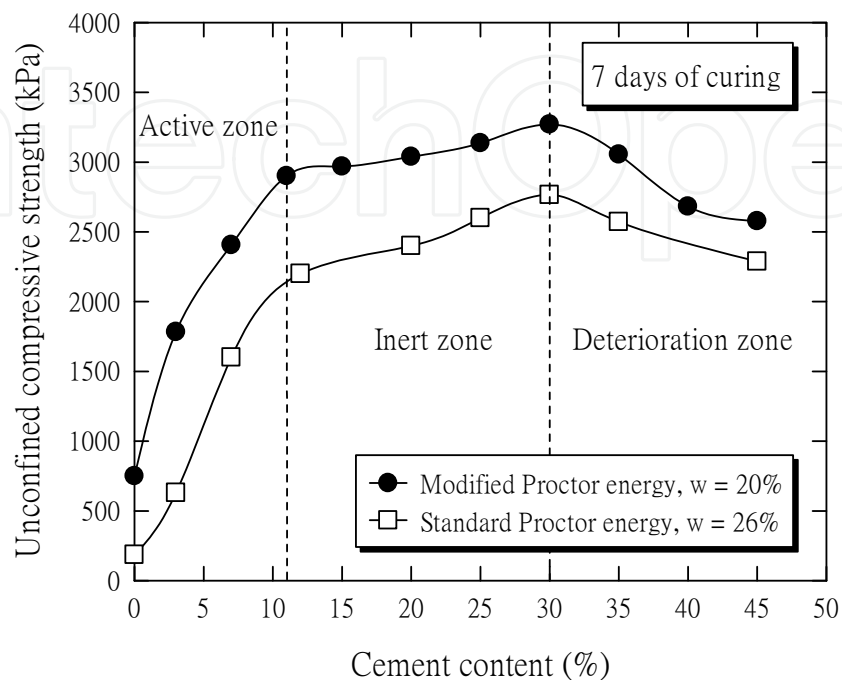


Fig. 5. Strength development as a function of cement content (Horpibulsuk et al., 2010b)

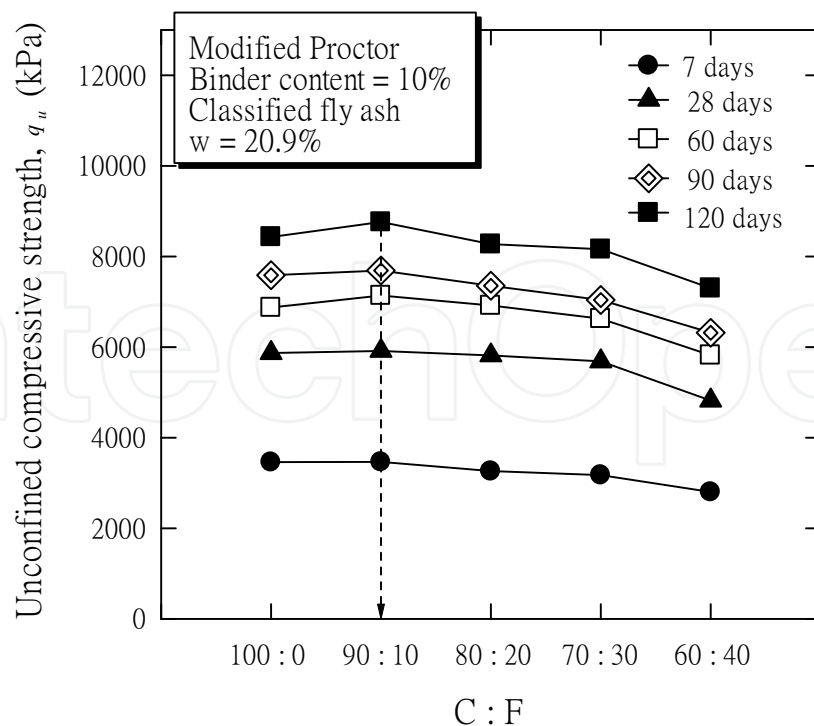


Fig. 6. Relationship between strength development and replacement ratio of the CFA blended cement stabilized clay at different curing times (Horpibulsuk et al., 2009)

### 3. Microstructure of cement stabilized clay

#### 3.1 Unstabilized clay

For compacted fine-grained soils, the soil structure mainly controls the strength and resistance to deformation, which is governed by compaction energy and water content. Compaction breaks down the large clay clusters into smaller clusters and reduces the pore space. Figure 7 shows SEM photos of the unstabilized samples compacted under the modified Proctor energy at water contents in the range of 0.8OWC to 1.2OWC. On the wet side of optimum (*vide* Figure 7c), a dispersed structure is likely to develop because the quantity of pore water is enough to develop a complete double layer of the ions that are attracted to the clay particles. As such, the clay particles and clay clusters easily slide over each other when sheared, which causes low strength and stiffness. On the dry side of optimum (*vide* Figure 7a), there is not sufficient water to develop a complete double-layer; thus, the distance between two clay platelets is small enough for van der Waals type attraction to dominate. Such an attraction leads to flocculation with more surface to edge bonds; thus, more aggregates of platelets lead to compressible flocs, which make up the overall structure. At the OWC, the structure results from a combination of these two characteristics. Under this condition, the compacted sample exhibits the highest strength and stiffness.

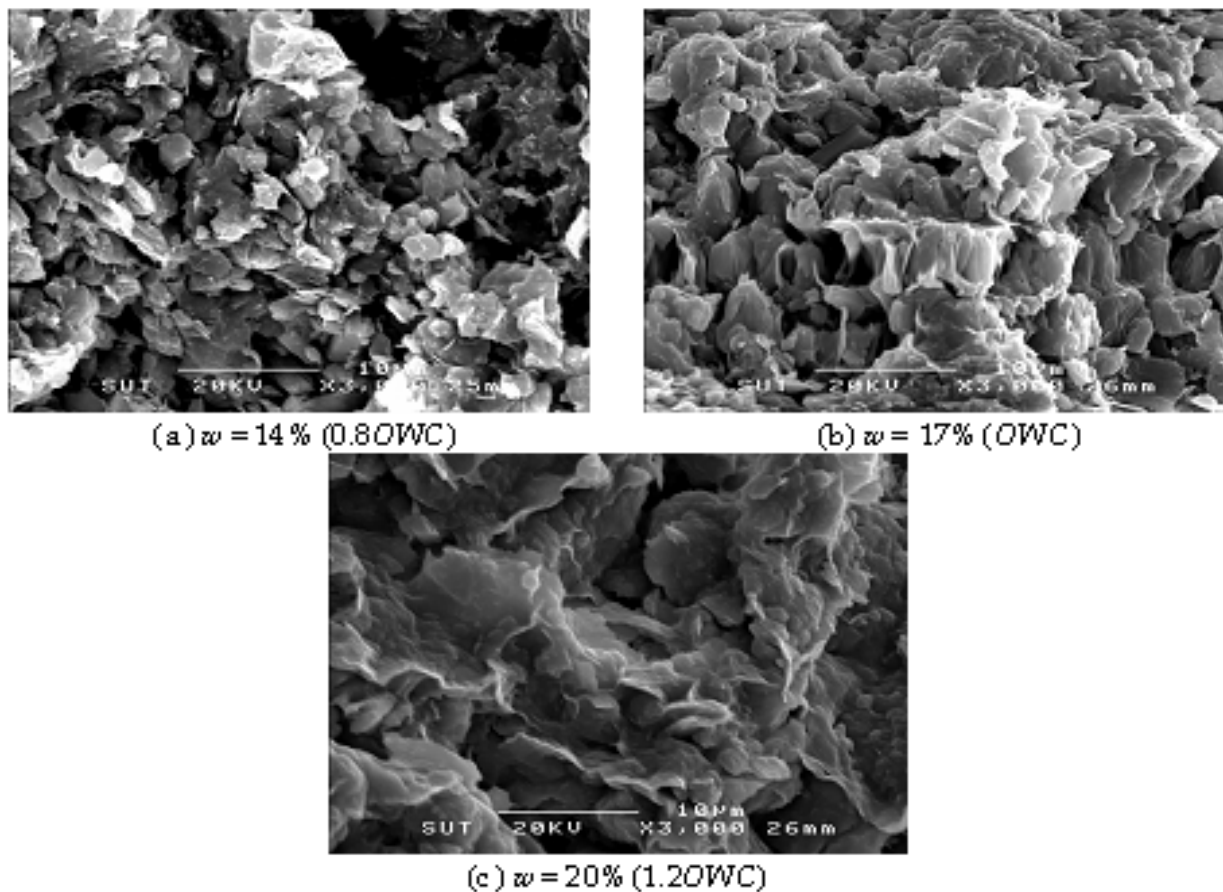


Fig. 7. SEM photos of the uncemented samples compacted at different molding water contents under modified Proctor energy (Horpibulsuk et al., 2010b)

### 3.2 Stabilized clay

#### 3.2.1 Effect of curing time

Figure 8 shows SEM photos of the 10% cement samples compacted at  $w = 20\%$  (1.2OWC) under the modified Proctor energy and cured for different curing times. After 4 hours of curing, the soil clusters and the pores are covered and filled by the cement gel (hydrated cement) (*vide* Figure 8a). Over time, the hydration products in the pores are clearly seen and the soil-cement clusters tend to be larger (*vide* Figures 8b through d) because of the growth of cementitious products over time (*vide* Table 2).

The effect of curing time on the pore size distribution of the stabilized samples is illustrated in Figure 9. It is found that, during the early stage of hydration (fewer than 7 days of curing), the volume of pores smaller than 0.1 micron significantly decreases while the volume of pores larger than 0.1 micron slightly increases. This result shows that during 7 days of curing, the cementitious products fill pores smaller than 0.1 micron and the coarse particles (unhydrated cement particles) cause large soil-cement clusters and large pore space. After 7 days of curing, the volume of pores larger than 0.1 micron tends to decrease while the volume of pores smaller than 0.1 micron tends to increase possibly because the cementitious products fill the large pores (larger than 0.1 micron). As a result, the volume of small pores (smaller than 0.1 micron) increases, and the total pore volume decreases.

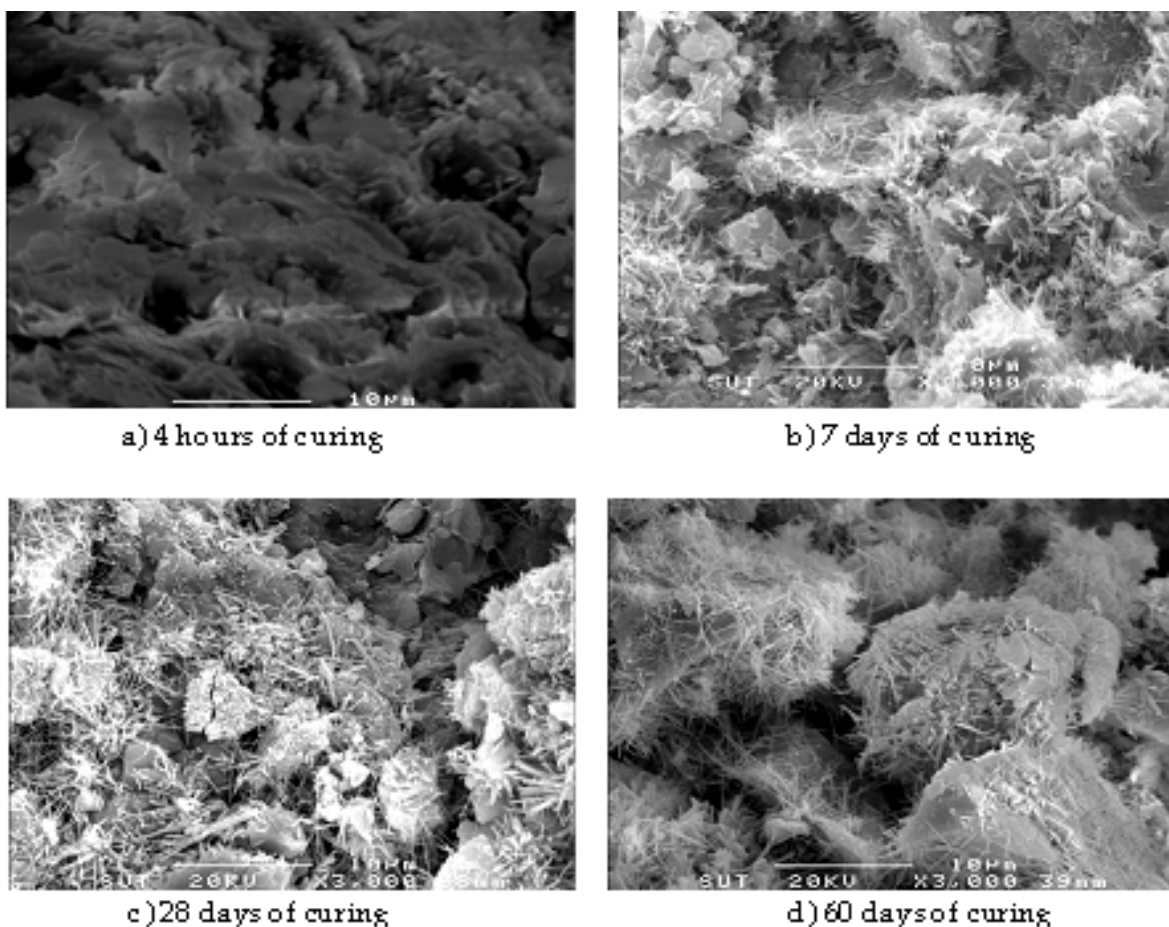


Fig. 8. SEM photos of the 10% cement samples compacted at 1.2OWC under modified Proctor energy at different curing times (Horpibulsuk et al., 2010b)

Curing time (days)	Weight loss (%)	Ca(OH) <sub>2</sub> (%)
7	1.52	6.25
28	1.65	6.78
60	1.85	7.63

Table 2. Ca(OH)<sub>2</sub> of the 10% cement samples compacted at 1.2OWC at different curing times under modified Proctor energy (Horpibulsuk et al., 2010b)

### 3.2.2 Effect of cement content

Figures 10 and 11 and Table 3 show the SEM photos, pore size distribution, and the amount of Ca(OH)<sub>2</sub> of the stabilized samples compacted at  $w = 20\%$  under the modified Proctor energy for different cement contents after 7 days of curing. Figures 10a-c, 10d-g, and 10h-j show SEM photos of the cemented samples in the active, inert, and deterioration zones, respectively. The SEM photo of the 3% cement sample (Figure 10a) is similar to that of the unstabilized sample because the input of cement is insignificant compared to the soil mass. As the cement content increases in the active zone, hydration products are clearly seen in the pores (*vide* Figures 10b and c) and the cementitious products significantly increase (Table 3).

The cementitious products not only enhance the inter-cluster bonding strength but also fill the pore space, as shown in Figure 11: the volume of pores smaller than 0.1 micron is significantly reduced with cement, thus, the reduction in total pore volume. As a result, the strength significantly increases with cement. For the inert zone, the presence of hydration products (Figures 10d to g) and cementitious products (Table 3) is almost the same for 15-30% cement. This results in an insignificant change in the pore size distribution and, thus, the strength. For the deterioration zone (Figure 10h-j), few hydration products are detected. Both the volumes of the highest pore size interval (1.0-0.1 micron pores) and the total pore tend to increase with cement (Figure 11). This is because the increase in cement content significantly reduces the water content, which decreases the degree of hydration and, thus, cementitious products (Table 3).

### 3.2.3 Effect of fly ash

Figures 12 and 13 show SEM photos of the CFA blended cement stabilized clay compacted at  $w = 1.2OWC$  ( $w = 20.9\%$ ) and cured for 28 and 60 days at different replacement ratios. The fly ash particles are clearly shown among clay-cement clusters especially for 30% replacement ratio (C:F = 70:30) for both curing times (Figures 12a and 13a). It is noted that the hydration products growing from the cement grains connect fly ash particles and clay-cement clusters together. Some of the surfaces of fly ash particles are coated with layers of amounts of hydration products. However, they are still smooth with different curing times. This finding is different from concrete technology where the precipitation in the pozzolanic reaction is indicated by the etching on fly ash surface (Fraay et al., 1989; Berry et al., 1994; Xu and Sarker, 1994; and Chindapasirt et al., 2005). This is because the input of cement in concrete is high enough to produce a relatively high amount of Ca(OH)<sub>2</sub> to be consumed for pozzolanic reaction. Its water to binder ratio ( $W/B$ ) is generally about 0.2-0.5, providing strength higher than 30 MPa (30,000 kPa) at 28 days of curing, whereas for ground improvement, the  $W/B$  is much lower. From this observation, it is thus possible to conclude that the pozzolanic reaction is minimal for strength development in the blended cement stabilized clay.

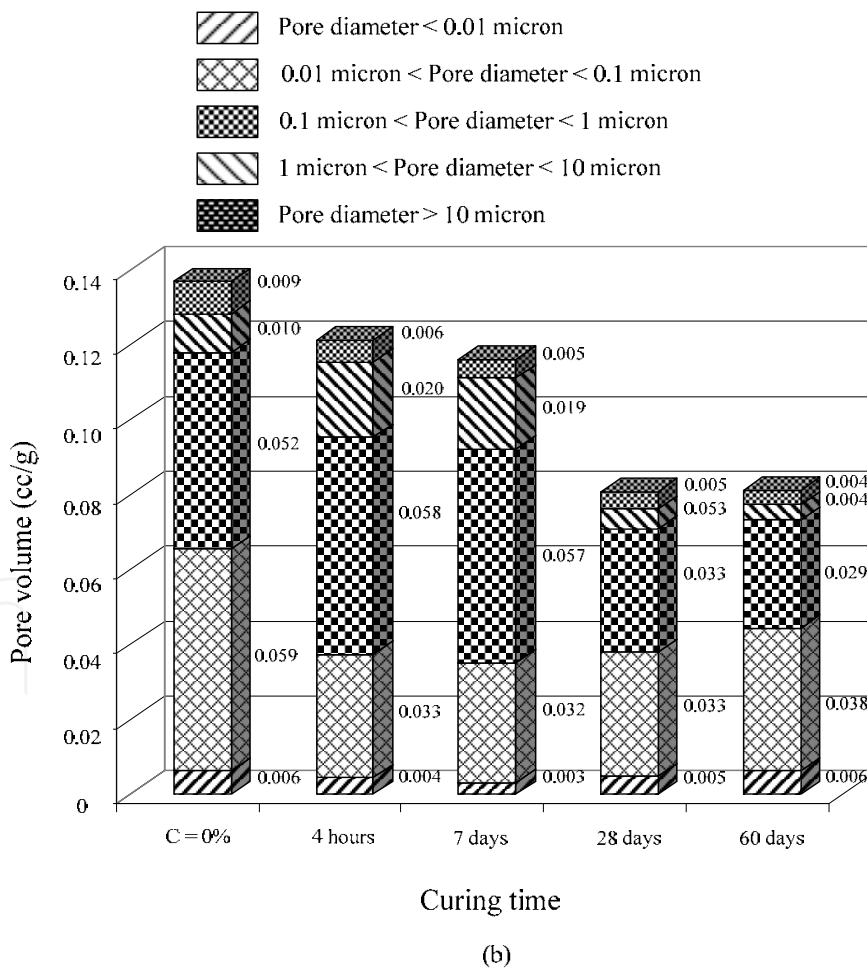
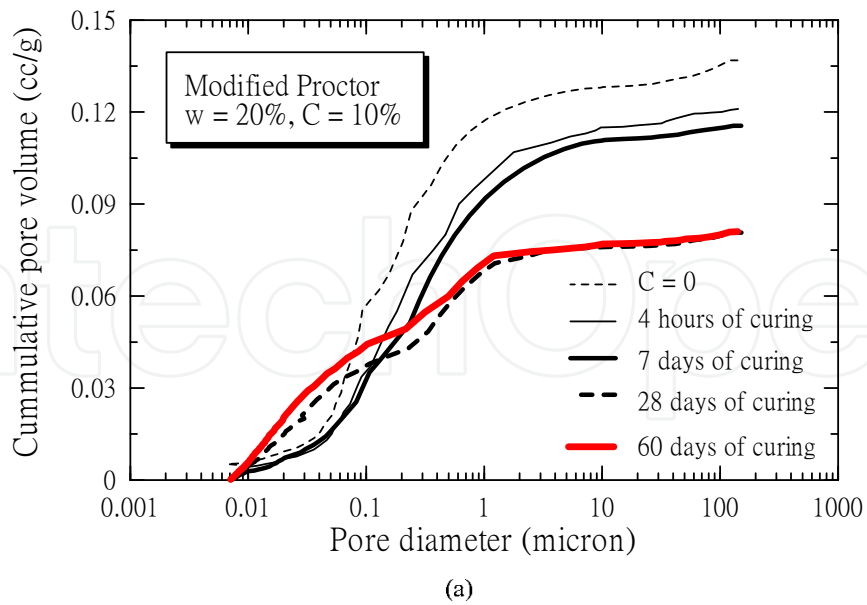


Fig. 9. Pore size distribution of the 10% cement samples compacted at different curing times under modified Proctor energy after 7 days of curing (Horpibulsuk et al., 2010b)

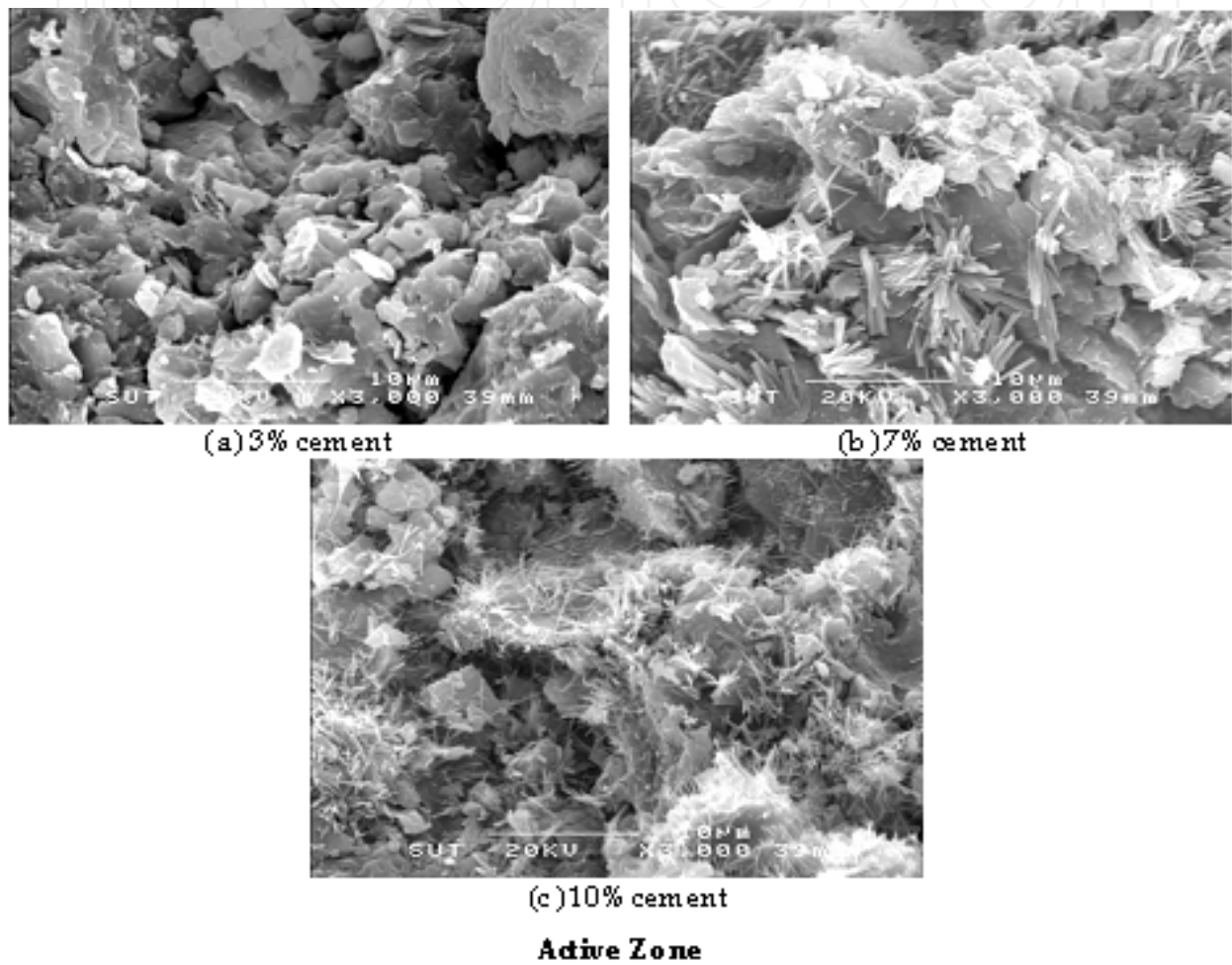


Fig. 10. SEM photos of the cemented samples compacted at different cement contents under modified Proctor energy after 7 days of curing (Horpibulsuk et al., 2010b)

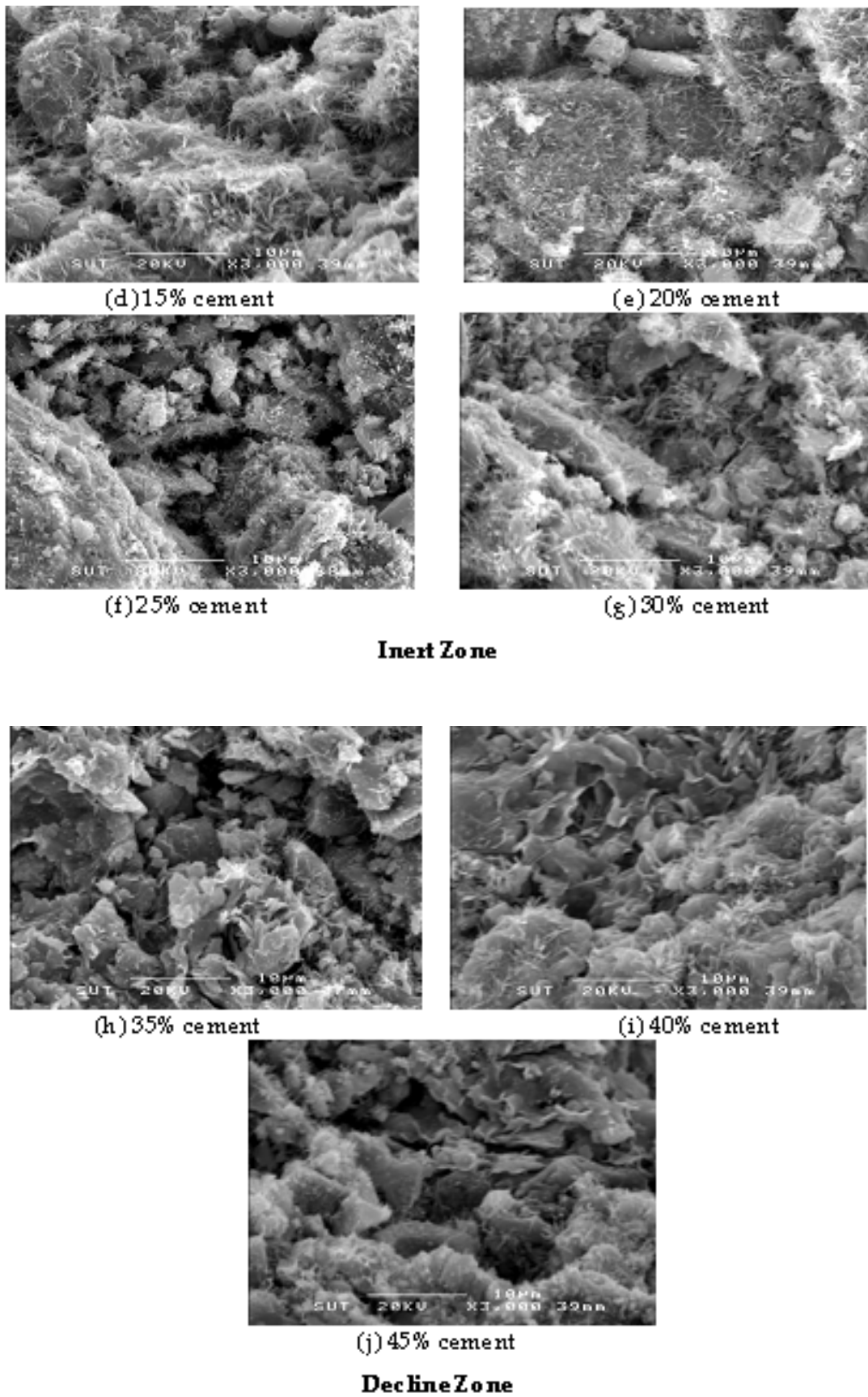


Fig. 10. (Continued)

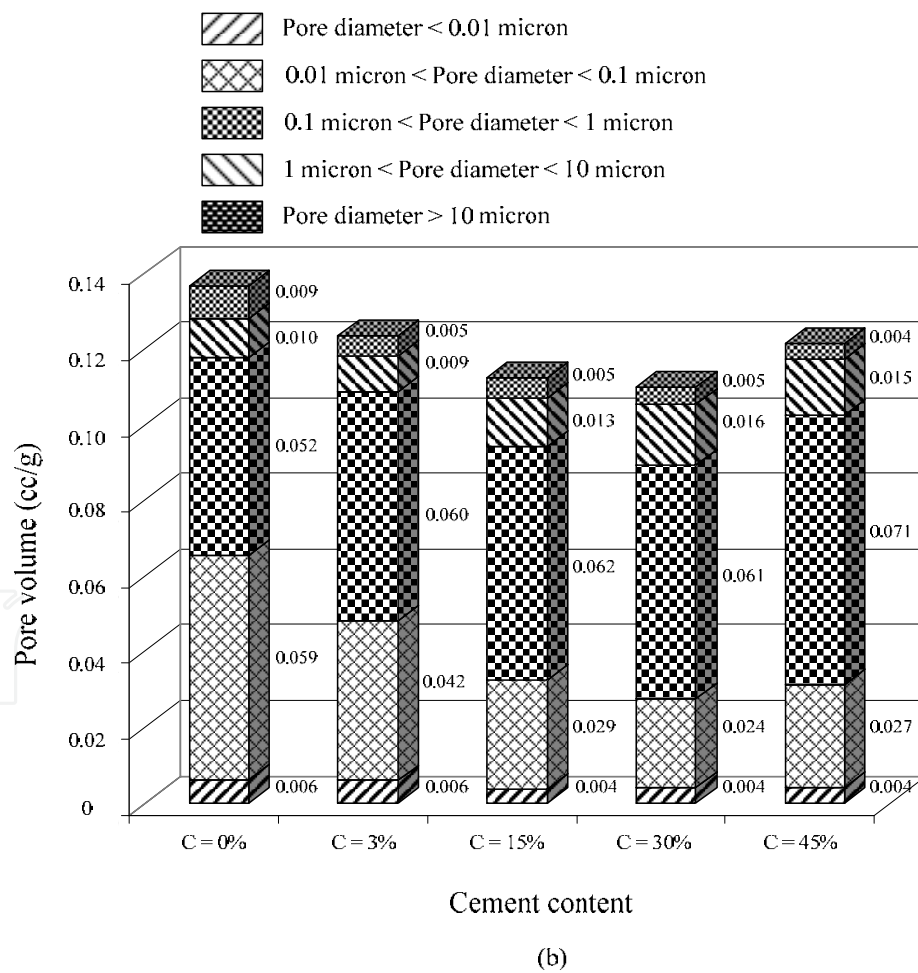
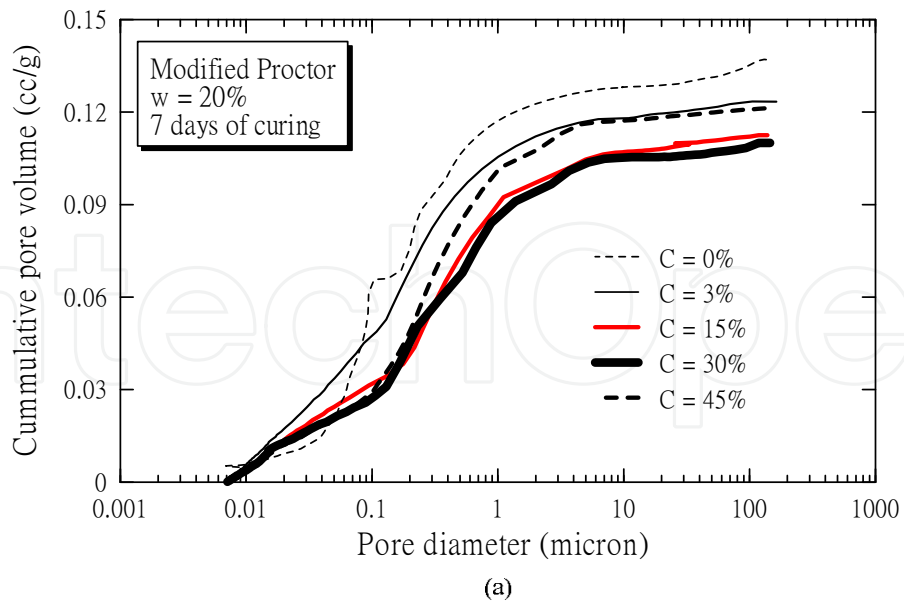


Fig. 11. Pore size distribution of the cemented samples compacted at different water contents and under modified Proctor energy after 7 days of curing time (Horpibulsuk et al., 2010b)

Improvement zones	Cement (%)	Weight loss (%)	Ca(OH) <sub>2</sub> (%)
Active	3	1.34	5.51
	7	1.50	6.17
	11	1.60	6.58
Inert	15	1.62	6.66
	20	1.65	6.78
	30	1.68	6.90
Deterioration	35	1.54	6.33
	40	1.48	6.08
	45	1.37	5.63

Table 3. Ca(OH)<sub>2</sub> of the cemented samples compacted at different cement contents under modified Proctor energy after 7 days of curing.

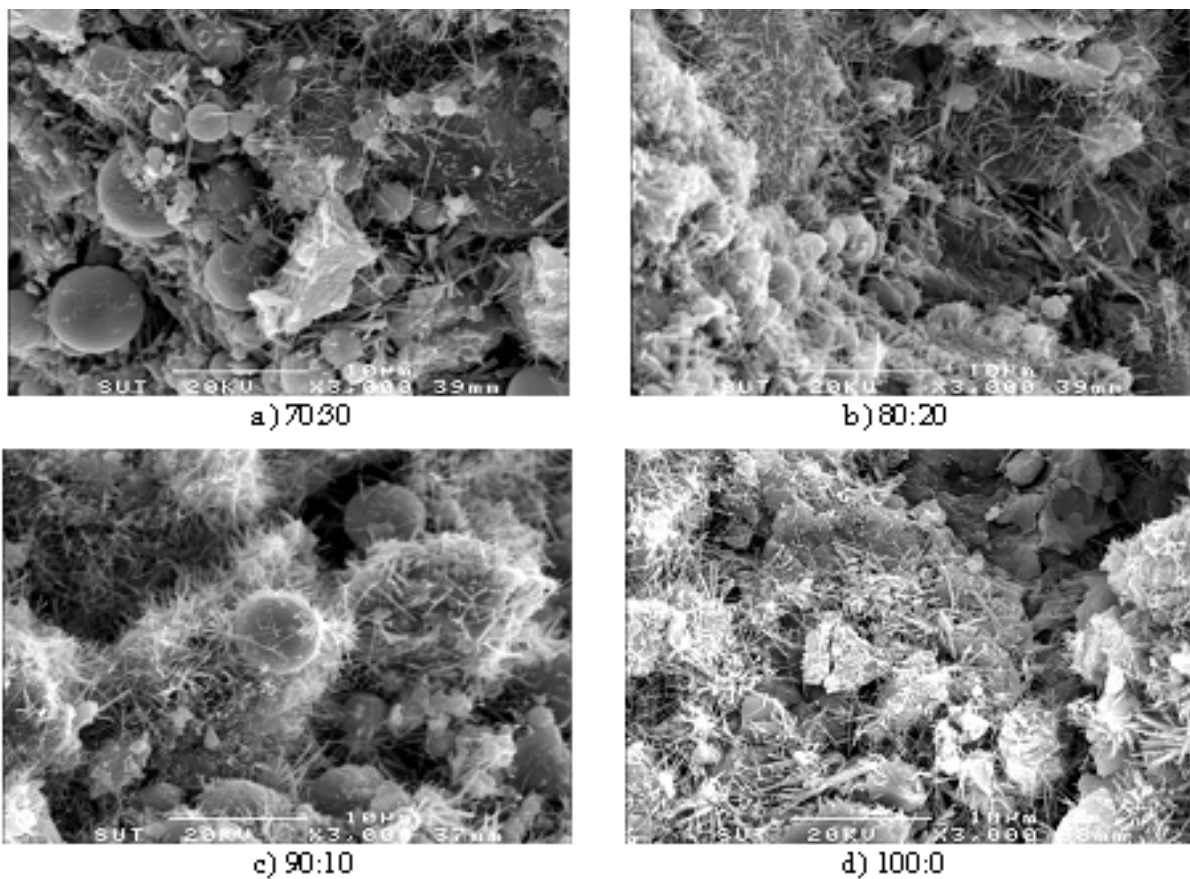


Fig. 12. SEM photos of the blended cement stabilized clay at different replacement ratios after 28 days of curing (Horpibulsuk et al., 2009)

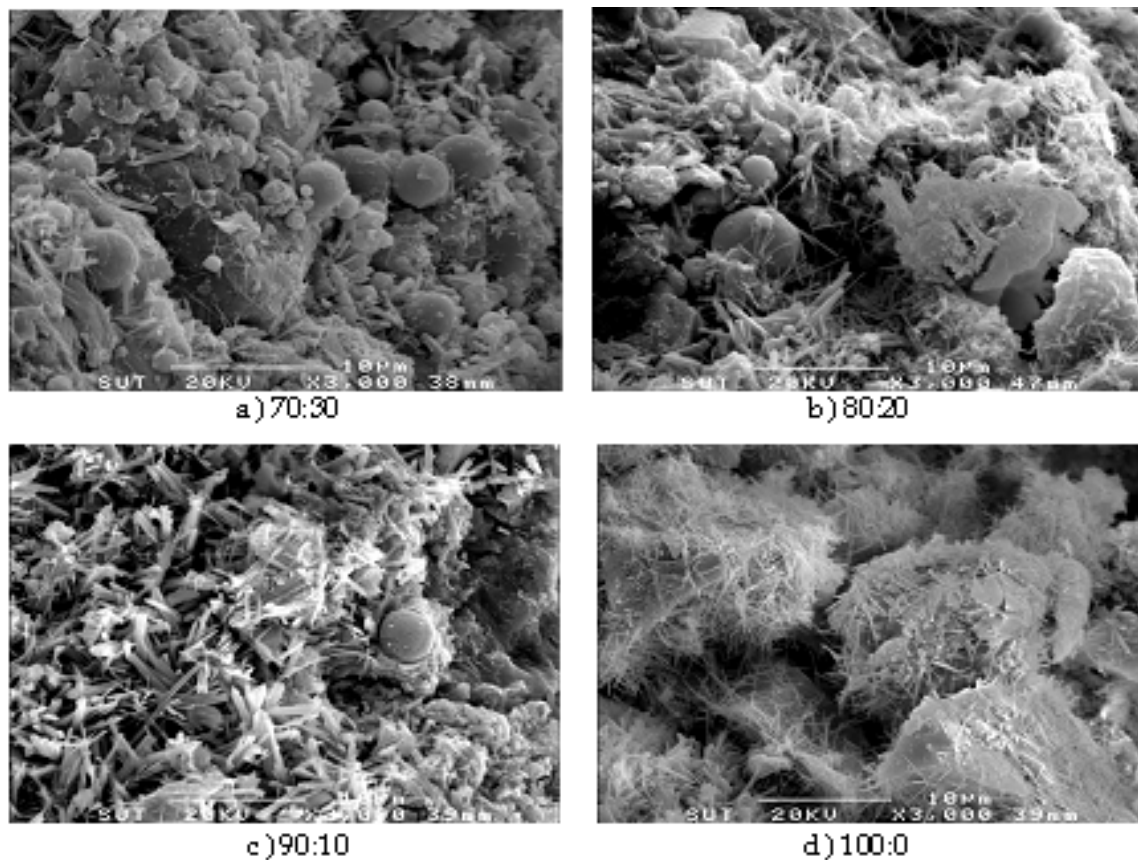
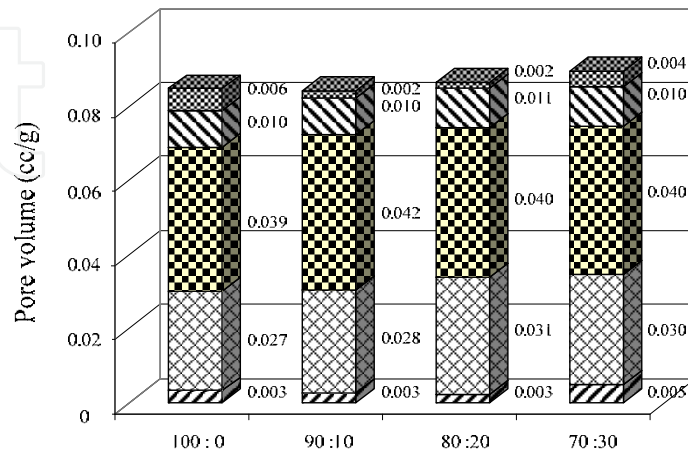


Fig. 13. SEM photos of the blended cement stabilized clay at different replacement ratios after 60 days of curing (Horpibulsuk et al., 2010b)

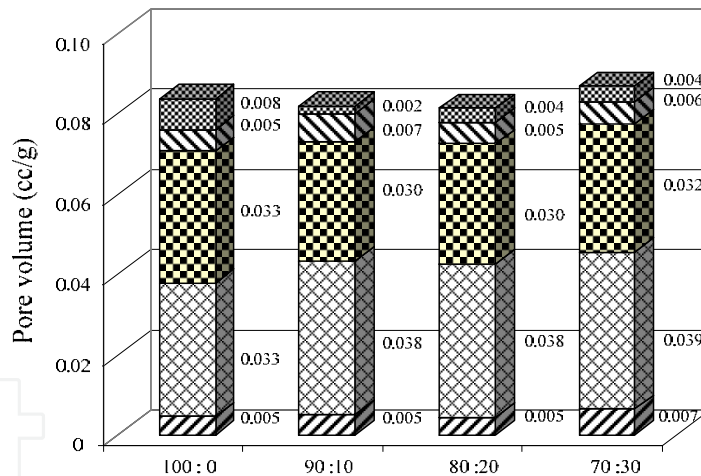
Figure 14 shows the pore size distribution of the CFA blended cement stabilized clay at different curing times and replacement ratios. The pore size distribution for all replacement ratios is almost identical since the grain size distribution and  $D_{50}$  of PC and CFA are practically the same. This implies that the strength of blended cement stabilized clay is not directly dependent upon only pore size distribution. However, it might control permeability and durability. With time, the total pore and large pore ( $>0.1$  micron) volumes decrease while the small pore ( $<0.1$  micron) volume increases. This is due to the growth of cementitious products filling up pores.

Table 4 shows  $\text{Ca(OH)}_2$  of the blended cement stabilized clay at  $w = 1.2\text{OWC}$  for different curing times. For a particular water content and curing time,  $\text{Ca(OH)}_2$  for the CFA blended cement stabilized clay decreases with replacement ratio only when the replacement ratio is in excess of a certain value. This finding is different from concrete technology in which  $\text{Ca(OH)}_2$  decreases significantly with the increase in fineness and replacement ratio (Berry et al., 1989; Sybertz and Wiens, 1991; and Harris et al., 1987; and Chindapasirt et al., 2005 and 2006; and others) due to pozzolanic reaction. The highest  $\text{Ca(OH)}_2$  is at 10% replacement ratio (C:F = 90:10) for all curing times. For replacement ratios higher than 10%,  $\text{Ca(OH)}_2$  decreases with replacement ratio.  $\text{Ca(OH)}_2$  at 20% replacement ratio is almost the same as that at 0% replacement ratio. This finding is associated with the strength test results that the 10% replacement ratio gives the highest strength and the strengths for 0% and 20% replacement ratios are practically the same for all curing times. It is thus concluded that

cementitious products mainly control the strength development. In other words, the strengths of the blended cement stabilized clay having different mixing condition (binder content, replacement ratios, and curing time) could be identical as long as cementitious products are the same.



C:F  
(a) 7 days



C:F  
(b) 28 days

- Pore diameter < 0.01 micron
- 0.01 micron < Pore diameter < 0.1 micron
- 0.1 micron < Pore diameter < 1 micron
- 1 micron < Pore diameter < 10 micron
- Pore diameter > 10 micron

Fig. 14. Pore size distribution of the blended cement stabilized clay at different replacement ratios and curing times (Horpibulsuk et al., 2010b)

Curing time (days)	Replacement ratio C : F	Fly ash	Ca(OH) <sub>2</sub> (%)		
			Test (Combined effect)	Hydration	Induced (dispersion effect)
7	100:0	-	6.67	6.67	0.00
	90:10	CFA	6.97	6.00	0.97
	80:20	CFA	6.79	5.34	1.45
	70:30	CFA	6.39	4.67	1.72
28	100:0	-	6.79	6.79	0.00
	90:10	CFA	6.96	6.11	0.85
	80:20	CFA	6.81	5.43	1.38
	70:30	CFA	6.57	4.75	1.82
60	100:0	-	6.82	6.82	0.00
	90:10	CFA	7.16	6.14	1.02
	80:20	CFA	6.92	5.46	1.46
	70:30	CFA	6.68	4.77	1.91
90	100:0	-	7.07	7.07	0.00
	90:10	CFA	7.28	6.36	0.91
	80:20	CFA	6.94	5.66	1.28
	70:30	CFA	6.67	4.95	1.72
120	100:0	-	7.08	7.08	0.00
	90:10	CFA	7.29	6.37	0.92
	80:20	CFA	6.96	5.66	1.30
	70:30	CFA	6.70	4.96	1.74

Table 4. Ca(OH)<sub>2</sub> of the blended cement stabilized clay at different replacement ratios and curing times.

From SEM and MIP observation, it is notable that the small pore (<0.1 micron) volumes of the blended cement stabilized clay are higher than those of the cement stabilized clay. This implies that a number of large clay-cement clusters possessing large pore space reduce

when fly ashes are utilized. In other words, the fly ashes disperse large clay-cement clusters into small clusters, resulting in the increase in small pore volume. The higher the replacement ratio, the better the dispersion. Consequently, the reactive surfaces increase, resulting in the increase in cementitious products as illustrated by dispersion induced  $\text{Ca(OH)}_2$  (*vide* Table 4). It is the difference in  $\text{Ca(OH)}_2$  of the blended cement stabilized clay due to the combined effect (hydration and dispersion) and due to hydration.  $\text{Ca(OH)}_2$  due to combined effect is directly obtained from TG test on the blended cement stabilized sample.  $\text{Ca(OH)}_2$  due to hydration is also obtained from TG test on the cement stabilized sample having the same cement content as the blended cement stabilized sample. For simplicity,  $\text{Ca(OH)}_2$  due to hydration at any cement content can be estimated from known  $\text{Ca(OH)}_2$  of cement stabilized clay at a specific cement content by assuming that the change in the cementitious products is directly proportional to the input of cement (Sinsiri et al., 2006). Thus,  $\text{Ca(OH)}_2$  due to hydration ( $H$ ) for any replacement ratio at a particular curing time is approximated in the form.

$$H = T \times (1 - F / 100) \quad (3)$$

where  $T$  is known  $\text{Ca(OH)}_2$  of the cement stabilized clay (0% replacement ratio) obtained from TG test, and  $F$  is the replacement ratio expressed in percentage. Sinsiri et al. (2006) have shown that  $\text{Ca(OH)}_2$  of the cement paste with fly ash is always lower than  $\text{Ca(OH)}_2$  of the cement paste without fly ash, resulted from  $\text{Ca(OH)}_2$  consumption for pozzolanic reaction. The same is not for the blended cement stabilized clay. It is found that  $\text{Ca(OH)}_2$  due to combined effect is higher than that due to hydration for all replacement ratios and curing times. The dispersion induced  $\text{Ca(OH)}_2$  increases with the replacement ratio for all curing times.

#### 4. Conclusions

This chapter presents the role of curing time, cement content and fly ash content on the strength and microstructure development in the cement stabilized clay. The following conclusions can be advanced:

1. The strength development with cement content for a specific water content is classified into three zones: active, inert and deterioration. In the active zone, the volume of pores smaller than 0.1 micron significantly decreases with the addition of cement because of the increase in cementitious products. In the inert zone, both pore size distribution and cementitious products change insignificantly with increasing cement; thus, there is a slight change in strength. In the deterioration zone, the water is not adequate for hydration because of the excess of cement input. Consequently, as cement content increases, the cementitious products and strength decreases.
2. The flocculation of clay particles due to the cation exchange process is controlled by cement content, regardless of fly ash content. It results in the increase in dry unit weight with insignificant change in liquid limit. Hence, OWCs of stabilized and unstabilized silty clay (low swelling clay) are practically the same.
3. The surfaces of fly ash in the blended cement stabilized clay are still smooth for different curing times and fineness, suggesting that pozzolanic reaction is minimal. Fly ash is considered as a dispersing material in the blended cement stabilized clay. This is

different from the application of fly ash as a pozzolanic material in concrete structure in which  $\text{Ca}(\text{OH})_2$  from hydration is much enough to be consumed for pozzolanic reaction.

4. From the microstructural investigation, it is concluded that the role of fly ash as a non-interacting material is to disperse the cement-clay clusters with large pore space into smaller clusters with smaller pore space. The dispersing effect by fly ash increases the reactive surfaces, and hence the increase in degree of hydration as clearly illustrated by the increase in the induced  $\text{Ca}(\text{OH})_2$  with replacement ratio and fineness.
5. The increase in cementitious products with time is observed from the scanning electron microscope, mercury intrusion porosimetry and thermal gravity test. With time, the large pore ( $>0.1$  micron) and total pore volumes decrease while the small pore ( $<0.1$  micron) volumes increase. This shows the growth of the cementitious products filling up the large pores.

## 5. Acknowledgment

This work was a part of the author's researches conducted in the Suranaree University of Technology. The authors would like to acknowledge the financial support provided by the Higher Education Research Promotion and National Research University Project of Thailand, Office of Higher Education Commission, the Thailand Research Fund (TRF), and the Suranaree University of Technology. The author is indebted to Dr. Theerawat Sinsiri, School of Civil Engineering, Suranaree University of Technology for his technical advice in cement and concrete technology. The author is grateful to Mr. Yutthana Raksachon, ex-master's student for his assistance.

## 6. References

- Berry, E.E., Hemmings, R.T., Langley, W.S. & Carette, G.G. (1989). Beneficiated Fly Ash: Hydration, Microstructure, and Strength Development in Portland Cement Systems, in: V.M. Malhotra (Ed.), *Third CANMET/ACI, Conference on Fly Ash, Silica Fume, Slag, and Natural Pozzolans in Concrete (SP-114)*, Detroit, pp.241-273.
- Chindaprasirt, P., Jaturapitakkul, C. & Sinsiri, T. (2005). Effect of Fly Ash Fineness on Compressive Strength and Pore Size of Blended Cement Plates. *Cement and Concrete Composites*, Vol.27, pp.425-258.
- Clough, G.W., Sitar, N., Bachus, R.C. & Rad, N.S. (1981). Cemented Sands under Static Loading. *Journal of Geotechnical Engineering Division, ASCE*, Vol.107, No.GT6, pp.799-817.
- El-Jazairi, B. & Illston, J.M. (1977). A Simultaneous Semi-Isothermal Method of Thermogravimetry and Derivative Thermogravimetry, and Its Application to Cement Plates. *Cement and Concrete Research*, Vol.7, pp.247-258.
- El-Jazairi, B. & Illston, J.M. (1980). The Hydration of Cement Plate Using the Semi-Isothermal Method of Thermogravimetry. *Cement and Concrete Research*, Vol.10, pp.361-366.
- Fraay, A.L.A, Bijen, J.M. & de Haan, Y.M. (1989). The Reaction of Fly Ash in Concrete: A Critical Examination. *Cement and Concrete Research*, Vol.19, pp.235-246.

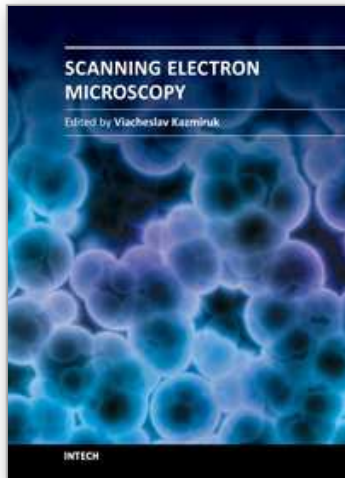
- Gens, A. & Nova, R. (1993). Conceptual Bases for Constitutive Model for Bonded Soil and Weak Rocks, *Geotechnical Engineering of Hard Soil-Soft Rocks*, Balkema.
- Kamon, M. & Bergado, D.T. (1992). Ground Improvement Techniques, *Proceedings of 9th Asian Regional Conference on Soil Mechanics and Foundation Engineering*, pp.526-546.
- Kasama, K., Ochiai, H. & Yasufuku, N. (2000). On the Stress-Strain Behaviour of Lightly Cemented Clay Based on an Extended Critical State Concept. *Soils and Foundations*, Vol.40, No.5, pp.37-47.
- Harris, H.A., Thompson, J.L. & Murphy, T.E. (1987). Factor Affecting the Reactivity of Fly Ash from Western Coals. *Cement and Concrete Aggregate*, Vol.9, pp.34-37.
- Horpibulsuk, S. & Miura, N. (2001). A new approach for studying behavior of cement stabilized clays, *Proceedings of 15th international conference on soil mechanics and geotechnical engineering (ISSMGE)*, pp. 1759-1762, Istanbul, Turkey.
- Horpibulsuk, S., Miura, N. & Nagaraj, T.S. (2003). Assessment of Strength Development in Cement-Admixed High Water Content Clays With Abrams' Law As a Basis. *Geotechnique*, Vol.53, No.4, pp.439-444.
- Horpibulsuk, S., Bergado, D.T. & Lorenzo, G.A. (2004a) Compressibility of Cement Admixed Clays at High Water Content. *Geotechnique*, Vol.54, No.2, pp.151-154.
- Horpibulsuk, S., Miura, N. & Bergado, D.T. (2004b). Undrained Shear Behavior of Cement Admixed Clay at High Water Content. *Journal of Geotechnical and Geoenvironmental Engineering*, ASCE, Vol.30, No.10, pp.1096-1105.
- Horpibulsuk, S., Miura, N., Koga, H. & Nagaraj, T.S. (2004c). Analysis of Strength Development in Deep Mixing - A Field Study. *Ground Improvement Journal*, Vol.8, No.2, pp.59-68.
- Horpibulsuk, S., Miura, N. & Nagaraj T.S. (2005). Clay-Water/Cement Ratio Identity of Cement Admixed Soft Clay. *Journal of Geotechnical and Geoenvironmental Engineering*, ASCE, Vol.131, No.2, pp.187-192.
- Horpibulsuk, S., Katkan, W., Sirilerdwattana, W. & Rachan, R. (2006). Strength Development in Cement Stabilized Low Plasticity and Coarse Grained Soils : Laboratory and Field Study. *Soils and Foundations*, Vol.46, No.3, pp.351-366.
- Horpibulsuk, S., Katkan, W. & Apichatvullop, A. (2008). An Approach for Assessment of Compaction Curves of Fine-Grained Soils at Various Energies Using a One Point Test. *Soils and Foundations*, Vol.48, No.1, pp.115-125.
- Horpibulsuk, S., Katkan, W. & Naramitkornburee, A. (2009). Modified Ohio's Curves: A Rapid Estimation of Compaction Curves for Coarse- and Fine-Grained Soils. *Geotechnical Testing Journal*, ASTM, Vol.32, No.1, pp.64-75.
- Horpibulsuk, S., Liu, M.D., Liyanapathirana, D.S. & Suebsuk, J. (2010a). Behavior of Cemented Clay Simulated via the Theoretical Framework of the Structured Cam Clay Model. *Computers and Geotechnics*, Vol.37, pp.1-9.
- Horpibulsuk, S., Rachan, R., Chinkulkijniwat, A., Raksachon, Y., and Suddeepong, A. (2010b). Analysis of Strength Development in Cement-Stabilized Silty Clay based on Microstructural Considerations. *Construction and Building Materials*, Vol.24, pp.2011-2021.

- Horpibulsuk, S., Rachan, R. & Suddeepong, A. (2011a). Assessment of Strength Development in Blended Cement Admixed Bangkok Clay. *Construction and Building Materials*, Vol.25, No.4, pp.1521-1531.
- Horpibulsuk, S., Rachan, R., Suddeepong, A. & Chinkulkijniwat, A. (2011b). Strength Development in Cement Admixed Bangkok Clay: Laboratory and Field Investigations. *Soils and Foundations*, Vol.51, No.2, pp.239-251.
- JEOL JSM-6400 (1989). Scanning Microscope Operations Manual, Model SM-6400 LOT No. SM150095, Copyright 1989, JEOL Ltd.
- Midgley, H.G. (1979). The Determination of Calcium Hydroxide in Set Portland Cements. *Cement and Concrete Research*, Vol.9, pp.77-82.
- Mitchell, J.K. (1993). *Fundamentals of Soil Behavior*. John Wiley&Sons, Inc., New York.
- Miura, N., Yamadera, A. & Hino, T. (1999). Consideration on Compression Properties of Marine Clay Based on the Pore Size Distribution Measurement. *Journal of Geotechnical Engineering*, JSCE.
- Miura, N., Horpibulsuk, S. & Nagaraj, T.S. (2001). Engineering Behavior of Cement Stabilized Clay at High Water Content. *Soils and Foundations*, Vol.41, No.5, pp.33-45.
- Nishida, K., Koga, Y. & Miura, N. (1996). Energy Consideration of the Dry Jet Mixing method, *Proceedings of 2nd International Conference on Ground Improvement Geosystems*, IS-Tokyo '96, Vol.1, pp.643-748.
- Sinsiri, T., Jaturapitakkul, C. & Chindaprasirt, P. (2006). Influence of Fly Ash Fineness on Calcium Hydroxide in Blended Cement Paste, *Proceedings of Technology and Innovation for Sustainable Development Conference (TISD2006)*, Khon Kaen University, Thailand.
- Suebsuk, J., Horpibulsuk, S. & Liu, M.D. (2010). Modified Structured Cam Clay: A Constitutive Model for Destructured, Naturally Structured and Artificially Structured Clays. *Computers and Geotechnics*, Vol.37, pp.956-968.
- Suebsuk, J., Horpibulsuk, S. & Liu, M.D. (2011). A Critical State Model for Overconsolidated Structured Clays. *Computers and Geotechnics*, Vol.38, pp.648-658.
- Sybert, F. & Wiens, U. (1991). Effect of fly ash fineness on hydration characteristics and strength development, *Proceedings of International Conference on Blended Cement in Construction*, pp.152-165, University of Sheffield, UK.
- Wang, K.S., Lin, K.L., Lee, T.Y. & Tzeng, B.Y. (2004). The Hydration Characteristics When  $C_2S$  Is Present in MSWI Fly Ash Slag. *Cement and Concrete Research*, Vol.26, pp.323-330.
- Washburn, E.W. (1921). Note on Method of Determining the Distribution of Pore Size in Porous Material, *Proceedings of the National Academy of Science*, USA. Vol.7, pp.115-116.
- Xu, A. & Sarker, S.L. (1994). Microstructure Development in High-Volume Fly Ash Cement System. *Journal of Material in Civil Engineering*, ASCE, Vol.6, pp.117-136.
- Yamadera, A. (1999). *Microstructural Study of Geotechnical Characteristics of Marine Clays*. Ph.D. Dissertation, Saga University, Japan.

Yin, J.H. & Lai, C.K. (1998). Strength and Stiffness of Hong Kong Marine Deposit Mixed With Cement. *Geotechnical Engineering Journal*. Vol.29, No.1, pp.29-44.

IntechOpen

IntechOpen



## **Scanning Electron Microscopy**

Edited by Dr. Viacheslav Kazmiruk

ISBN 978-953-51-0092-8

Hard cover, 830 pages

**Publisher** InTech

**Published online** 09, March, 2012

**Published in print edition** March, 2012

Today, an individual would be hard-pressed to find any science field that does not employ methods and instruments based on the use of fine focused electron and ion beams. Well instrumented and supplemented with advanced methods and techniques, SEMs provide possibilities not only of surface imaging but quantitative measurement of object topologies, local electrophysical characteristics of semiconductor structures and performing elemental analysis. Moreover, a fine focused e-beam is widely used for the creation of micro and nanostructures. The book's approach covers both theoretical and practical issues related to scanning electron microscopy. The book has 41 chapters, divided into six sections: Instrumentation, Methodology, Biology, Medicine, Material Science, Nanostructured Materials for Electronic Industry, Thin Films, Membranes, Ceramic, Geoscience, and Mineralogy. Each chapter, written by different authors, is a complete work which presupposes that readers have some background knowledge on the subject.

### **How to reference**

In order to correctly reference this scholarly work, feel free to copy and paste the following:

Suksun Horpibulsuk (2012). Strength and Microstructure of Cement Stabilized Clay, Scanning Electron Microscopy, Dr. Viacheslav Kazmiruk (Ed.), ISBN: 978-953-51-0092-8, InTech, Available from: <http://www.intechopen.com/books/scanning-electron-microscopy/strength-and-microstructure-of-cement-stabilized-clay>

**INTECH**  
open science | open minds

### **InTech Europe**

University Campus STeP Ri  
Slavka Krautzeka 83/A  
51000 Rijeka, Croatia  
Phone: +385 (51) 770 447  
Fax: +385 (51) 686 166  
[www.intechopen.com](http://www.intechopen.com)

### **InTech China**

Unit 405, Office Block, Hotel Equatorial Shanghai  
No.65, Yan An Road (West), Shanghai, 200040, China  
中国上海市延安西路65号上海国际贵都大饭店办公楼405单元  
Phone: +86-21-62489820  
Fax: +86-21-62489821

© 2012 The Author(s). Licensee IntechOpen. This is an open access article distributed under the terms of the [Creative Commons Attribution 3.0 License](#), which permits unrestricted use, distribution, and reproduction in any medium, provided the original work is properly cited.

IntechOpen

IntechOpen